Characterization of two low E_m forms of cytochrome a_3 and their carbon monoxide complexes in mammalian cytochrome *c* oxidase

Gurmel S. Sidhu and Richard W. Hendler
Laboratory of Cell Biology, National Heart, Lung, and Blood Institute, Bethesda, Maryland 20892 USA

ABSTRACT Evidence is presented for the existence of two forms of low-potential cytochrome a_3. One appears to be similar to the low-spin form reported by Nicholls, P., and V. Hildebrandt (1978. *Biochem. J.* 173:65–72) and Wrigglesworth, J. M., J. Elsden, A. Chapman, N. Van der Water, and M. F. Grahn (1988. *Biochim. Biophys. Acta.* 936:452–464). It has a reduced Soret peak near 428 nm and a prominent α peak near 602 nm. This form is seen when the enzyme is either supplemented with lipoprotein or incorporated into a liposomal membrane, preexposed to a voltage >400 mV for at least 30 min, and titrated in the presence of ~1 mM $K_3Fe(CN)_6$. The other form has a reduced Soret peak near 446 nm, and no prominent α peak. The 428-nm form has an E_m near 175 mV and forms a CO complex with an E_m near 225 mV. The 446-nm form has an E_m near 200 mV and forms a CO complex with an E_m near 335 mV.

INTRODUCTION

In a contemporary review on the structure and function of cytochrome *c* oxidase, Brunori et al. (1988) state that there is general agreement that the hemes display two n = 1 Nernstian transitions; one at ~360 mV and one at ~240 mV. In addition to the work from several laboratories cited in this review (Carithers and Palmer, 1981; Hartzell and Beinert, 1976; Schroedl and Hartzell, 1977; Lyndsay et al., 1975) there are many other papers which support the same conclusion (Wilson et al., 1972; Leigh et al., 1974; Tiesjema et al., 1973). Wikström et al. (1981) also state that the redox titration of cytochrome oxidase reveals two n = 1 Nernstian transitions for the hemes.

In nearly all of these studies the absorbance at a single wavelength or a pair of wavelengths, characteristic of a Soret or α peak of the enzyme was used to determine the extent of reduction at a particular voltage. With an assumed value for the amount of absorbance representative of 100% reduction, data were expressed as voltage vs. log (oxidized/reduced) and analyzed by a graphic procedure. Published work from our laboratory can also be added to the list cited above which found two equal n = 1 titrations for the hemes of cytochrome oxidase, when we ignored all of our collected spectral data except for the usual pairs of wavelengths used to analyze these titrations and when we applied the usual graphic method of analysis (Reddy et al., 1986; Hendler et al., 1986). The problem is that data in the form of a two-point ΔA and the graphic analytical method in common use cannot always resolve the mixture of Nernstian components which may be present (Shrager and Hendler, 1986). A complete analysis of the redox behavior of both pure cytochrome *c* oxidase and cytochrome *c* oxidase in mitochondria using a second derivative analysis centered on Soret and α peaks and using singular value decomposition analysis of entire optical spectra and analyzing series of both oxidative and reductive titrations in the range of 100 to 450 mV reveals (at least) three Nernstian titrations for the hemes (Hendler et al., 1986; Reddy et al., 1986). The E_m values are near 200, 260, and 340 mV and the n values are 2, 2, and 1, respectively. The lowest E_m represents two forms of cytochrome a_3 as described in this paper. The two higher E_m components represent different forms of cytochrome *a* and a reverse titration of a high potential form of cytochrome a_3 (Hendler et al., 1986; Hendler and Sidhu, 1988).

Our evidence for the existence of both a high- and a low-potential form of cytochrome a_3 and for the oxidation of the former as the ambient voltage is lowered from ~450 to ~200 mV supports a view of strong redox cooperativity between redox centers in cytochrome oxidase. The likelihood of redox cooperativity was recognized in the "neoclassical" model presented by Nicholls and Peterson (1974) and Malmström (1974) and Wikström et al. (1976). The neoclassical model, which considered only

High- and low-E_m species of cytochrome a_3 are designated as a_{3H} and a_{3L}, respectively. The distinction between the two low-E_m species of cytochrome a_3 utilizes the wavelengths of the major absorbance features. Thus, (428/602) refers to the low-spin form with a Soret peak at ~428 nm and an α peak at ~602 nm, whereas (446) refers to the high-spin species with a Soret peak near 446 nm and no prominent α feature.

two heme centers and two electrons, however, is not able to explain our newer findings nor those of others (Nicholls and Wrigglesworth, 1988).

The results presented in the present paper appear to support earlier findings of Nicholls and Hildebrandt (1978) and newer findings of Wrigglesworth et al. (1988) which indicate the existence of a low spin-activated form of cytochrome a_3. This form of the enzyme reported here, using a purified preparation, was also seen in intact mitochondria during potentiometric titrations (Reddy et al., 1986). Because of the overlap of Soret peaks in the mitochondria, only the characteristic α absorbance at 602 nm could be used. The E_m of this species, its convertibility to the CO form and the E_m of the CO-complex were the same as found with the purified enzyme either in a phospholipid-supplemented medium, or when the enzyme was incorporated into liposomes (Hendler et al., 1986).

EXPERIMENTAL PROCEDURES

General

The chemical sources, titration procedures, apparatus and general procedures have been previously described (Reddy and Hendler, 1986; Reddy et al., 1986; Hendler et al., 1986). The enzyme used for most of the studies was prepared from bovine heart muscle by the method of Yoshikawa et al. (1977) and was provided by Dr. Gary Yewey and Dr. Winslow Caughey. The preparations were 0.9–1.6 mM with respect to heme A, in 0.01 M sodium phosphate, pH 7.4, and 10–11 nmol heme A/mg protein (ϵ = 20 mM^{-1} cm^{-1}). The preparation has nine polypeptide chains, a metal stoichiometry of 5 Cu/4 Fe/2 Zn/2 Mg per dimer and is optically clear under experimental conditions. Recently this preparation of the enzyme has been crystallized and studied by x-ray diffraction (Yoshikawa et al., 1988). The concentrated enzyme was distributed in 10- or 20-μl aliquots and stored aerobically at −80°C. Confirmatory studies were performed with cytochrome oxidase prepared according to the procedure of Yonetani (1961) (gift of David Bickar).

Formation of low-potential cytochrome a_3 with a Soret peak near 428 nm and an α peak near 602 nm (a_{3L} [428/602])

Procedure a

Cytochrome aa_3 (6 μM heme A, 0.47 mg protein) was added to an aqueous medium containing 125 mM KCl, 62.5 mM potassium phosphate (pH = 7.0) and redox mediators: phenazine methosulfate, 1,2-naphthoquinone, and quinhydrone at 0.1 mM each; potassium ferricyanide (0.2 mM), and chicken whole egg homogenate (~13 mg protein) in a final volume of 3.0 ml. The cuvette was closed and continuously stirred while being flushed under an atmosphere of argon gas for at least 20 min. The voltage of the medium was raised electrically to 400 mV, and then 2–3 μl of 1 M $K_3Fe(CN)_6$ was added, followed by 20 μl (15 mM) diamodurene. The voltage was held at 465 mV for 30–60 min and then electrically reduced in steps to 260 mV over a period of ~20 min. After holding at 260 mV for 60 min, an electrical reductive titration to 95 mV in steps of 5 mV was conducted.

Procedure b

The above procedure was followed up to the point of holding the preparation at 260 mV for 60 min. Then 6 μl of 1 M $Na_2S_2O_4$ was added, reducing the voltage to ~ −100 mV, and the preparation was allowed to sit for 30 min. The voltage was raised electrically to 20 mV and held for 30 min and then to 100 mV and held for 90–120 min.

Formation of low-potential cytochrome a_3 with a Soret peak near 446 nm (a_{3L} [446])

Procedure a

The same procedure a described above for the formation of a_{3L} (428/602) was followed up to the point of flushing the closed cuvette with argon gas for at least 20 min. No additional $K_3Fe(CN)_6$ was added, nor egg homogenate, nor was the voltage raised to above 400 mV and held as described in the preparation of a_{3L} (428/602). The voltage of the solution at this point was ~270 mV. Then the preparation was reduced electrically down to 100 mV in steps of ~5 mV.

Procedure b

This procedure was sometimes used preparatory to the formation of the CO complex of a_{3L} (446) and its subsequent oxidation. It proved to be difficult to maintain the CO complex in its reduced form because of the pronounced tendency of $K_3Fe(CN)_6$, used in mediator concentration (0.2 mM), to oxidize the complex. It was necessary, therefore, to use an excess of $Na_2S_2O_4$ before the addition of the $K_3Fe(CN)_6$. In this procedure, the enzyme was added to the buffer without the mediators. After the cuvette was closed and flushed with argon, 8 μl of 1 M $Na_2S_2O_4$ was added to bring the voltage to −200 mV. The preparation was held for 10 min at −200 mV, and then all of the mediators, including $K_3Fe(CN)_6$, were added slowly while holding the voltage near −200 mV.

Formation of CO complexes of a_{3L} (428/602) and a_{3L} (446)

First either a_{3L} (428/602) or a_{3L} (446) was formed by one of the procedures described above. In the case of a_{3L} (428/602), the preparation was held at 100 mV for 60 min after switching from an argon to a CO atmosphere. In the case of a_{3L} (446), at the voltage specified, the atmosphere was switched from argon to CO and held for ~40 min. The rate of formation of a_{3L} (446) · CO was much faster than for a_{3L} (428/602) · CO. Usually ~90% was formed within 10 min.

Improvement in singular value decomposition (SVD) analysis

In previous applications of this method, the eigenvectors of the titration matrix were fitted individually to various Nernstian models of the titration. In the current work, all of the vectors were simultaneously fitted using the squares of the singular values as weighting factors. This procedure, while improving the quality of the "fits," also improves the objectivity of the process.

Comment on wavelength positions of absorbance features

The exact position of the Soret peak near 428 or 446 nm varies with different preparations of the enzyme to the extent of ~±1 nm. This

variability in the location of Soret maxima for preparations of cytochrome *c* oxidase from laboratory to laboratory and from preparation to preparation within a single laboratory has been noted, as well as a difference in reactivity towards CN^- and the presence of $g = 12$ ESR signal related to the conformation of the enzyme (Baker et al., 1987; Naqui et al., 1984). It is also true that calibrations of spectrometers in different laboratories could reasonably differ to the extent of $\sim \pm 1$ nm. Our spectrometer uses a 256 photodiode array as a detector with a resolution of 1.2 nm. For the above reasons, we state the position of the Soret peaks of interest as near 428 and near 446 nm rather than giving exact fixed wavelength positions. The phenomena we describe are not dependent on any more precise fixing of these peaks.

RESULTS

Demonstration of two forms of low potential cytochrome a_3

We have previously shown that a form of cytochrome a_3 exists which displays a Soret peak near 428 nm and an α peak at ~602 nm (428/602 species) (Hendler et al., 1986). The second derivative of absorbance vs. wavelength centered at 429 nm showed a Nernstian transition with an E_m value of 175 mV and an n value of 2. The difference spectrum for this transition showed a prominent shoulder near 446 nm on the Soret peak. When the titration was performed under a CO atmosphere, this spectral component was not seen. Instead a Soret peak near 433 nm and an α peak near 593 nm (433/593) was formed upon reduction. These are the spectral features characteristic of the CO-liganded form of cytochrome a_3 (Yoshikawa et al., 1977). The ability to convert the 428/602 species into the 433/593 species is the basis for the identification of the former as cytochrome a_3. To see the 428/602 species, a lipoprotein supplement, in the form of a raw hen egg homogenate, was required. In the absence of this addition, the Soret peak was shifted toward 446 nm. The characteristic wavelength maxima cited throughout this paper refer to reduced minus oxidized difference spectra. However, the predominant features at ~428, 446, 602, and 607 nm are also seen in absolute spectra (cf Fig. 3).

In Fig. 1, two titrations are shown, one conducted with hen egg homogenate present (panel *a*) and one where it was omitted (panel *b*). The second derivative of absorbance vs. wavelength centered at 428 nm (solid line) represents the 428/602 species of cytochrome a_3 as identified in titrations in the presence and absence of CO (Hendler et al., 1986). The second derivative centered at 446 nm represents cytochrome *a* above 200 mV, and the 446-nm species of cytochrome a_3 below 200 mV (Hendler et al., 1986). When egg homogenate was present (panel *a*) the titration below 200 mV was expressed mainly in the formation of the 428/602 species (a_{3L} [428/602]),

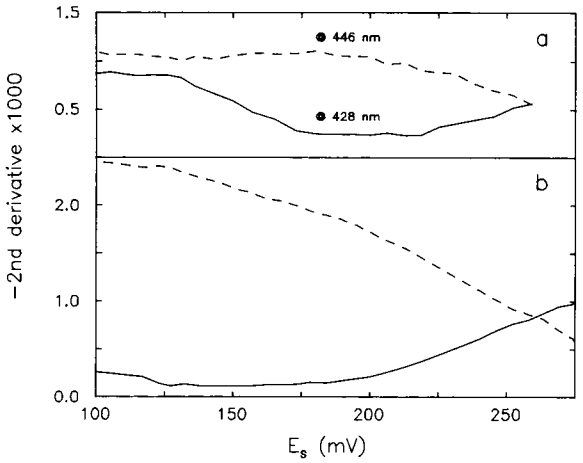

FIGURE 1 Cytochrome aa_3 (6 μM [heme A], 0.47 mg protein) in an aqueous medium containing 125 mM KCl, 62.5 mM potassium phosphate (pH 7.0) and the following redox mediators: phenazine methosulfate, 1,2-naphthoquinone, and quinhydrone at 0.1 mM each, and potassium ferricyanide at 0.2 mM was made anaerobic by flushing with argon gas for 25 min. (*a*) Hen egg homogenate (13 mg protein) was also present. The voltage was raised electrically to 400 mV, and 3 μL (1 M) $K_3Fe(CN)_6$ was added, followed by 20 μl (15 mM) diaminodurene. The voltage was then held at 465 mV for 30 min. The voltage was then electrically lowered in steps to 262 mV over a period of 19 min. After holding at 262 mV for 40–60 min, the preparation was subjected to an electrical reductive titration to 95 mV. The solid line shows the magnitude of the second derivative at 428 nm during the titration and the dashed line shows the magnitude of the second derivative at 446 nm. (*b*) No egg homogenate was present, the voltage was not raised to 465 mV, but the preparation was exposed briefly to its highest level of 296 mV, no additional supplement of 1 M $K_3Fe(CN)_6$ was provided. Electrical reduction was started immediately after adding the mediators and establishment of anaerobiosis. Solid and dashed lines have the same significance as in *a*.

whereas in the absence of the egg homogenate, the titration formed the 446 nm (a_{3L} [446]) species (panel *b*).

Complete spectral changes accompanying titrations in the presence and absence of egg homogenate are shown in Fig. 2. Panel *a* shows the difference spectrum (170–196 mV) obtained using a Yonetani preparation of cytochrome aa_3 in the presence of egg homogenate. The Soret region shows two peaks, the stronger one centered at ~428 nm and the weaker at ~446 nm. A very prominent α peak near 602 nm is also evident. In panel *b*, this transition is seen with more resolution as a result of an SVD deconvolution. In panel *c*, a difference spectrum (174–206 mV) obtained in the absence of egg homogenate is shown. There is none of the 428-nm species present. There is a much weaker α absorbance in the 600-610 nm range. The spectrum for this transition obtained by SVD is shown in panel *d*.

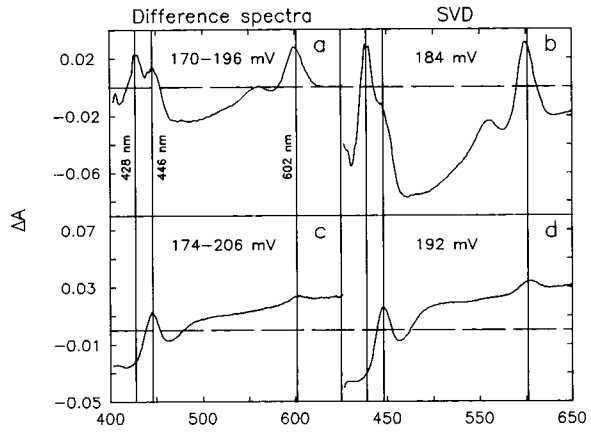

FIGURE 2 Difference spectra obtained from experiments conducted as described in the legend to Fig. 1 are presented. (*a*) A difference spectrum (170–196 mV) obtained using a Yonetani preparation of cytochrome aa_3 in a titration conducted under conditions described in Fig. 1 *a* (procedure a for a_{3L} (428/602) in Methods). (*b*) The SVD-deduced difference spectrum for this transition which the SVD analysis found to be at E_m = 184 mV. (*c*) Difference spectrum (175–206 mV) obtained in the titration described in Fig. 1 *b* (procedure b for a_{3L} (446) in Methods). (*d*) SVD-deduced difference spectrum for this titransition having an E_m = 192 mV. The vertical lines are drawn at 428, 446, and 602 nm.

Conditions that determine which form of low potential cytochrome a_3 is formed

Figs. 1 and 2 show that in the presence of egg homogenate, a 428/602 nm species of reduced cytochrome a_3 is favored but that in its absence only a 446 nm species is seen. We originally provided the egg supplement for two reasons. The extra protein was added to protect the pure cytochrome aa_3 from interfacial denaturation and the extra phospholipoprotein was added to provide a membrane-like environment for this integral membrane protein enzyme. In the earlier studies where the a_{3L} (428/602) species was first described, extra $K_3Fe(CN)_6$ (above the 0.2 mM mediator concentration) was added to raise the voltage of the solution to values above 400 mV. In newer studies, where higher E_m mediators than $K_3Fe(CN)_6$ were used, it was not necessary to use additional $K_3Fe(CN)_6$ to attain high voltages. When the enzyme was held at 468 mV for 1 h in the presence of 0.2 mM $K_3Fe(CN)_6$ and 0.04 mM $K_4W(CN)_8$, however, a_{3L} (428/602) was not seen, even in the presence of egg homogenate. Instead, only a_{3L} (446) was seen.

An extensive series of experiments was conducted to define conditions which favor the formation of the a_{3L} (428/602) species over the a_{3L} (446) form. It was found that to form appreciable amounts of the former, three conditions were important. (*a*) Egg homogenate must be present; (*b*) ~1 mM $K_3Fe(CN)_6$ must be present; (*c*) the enzyme must be preheld at a voltage >400 mV for a period of 30–60 min before the reductive titration.

Stability of the 428/602 nm species of cytochrome a_{3L} and the role of egg homogenate

A tentative conclusion drawn in the first paper in which the 428/602 species of cytochrome a_{3L} was described (Hendler et al., 1986) was that it was unstable. The basis of this view was that it was seen only in reductive titrations and only when egg homogenate was present, perhaps to stabilize the species. If the "labile" 428/602 species was generated upon reduction and if it decayed on a time scale of minutes, then during a reductive titration, it would be continuously regenerated as each new lower voltage was achieved. In an oxidative titration, the species would decay according to the time constant of its conversion to a more stable form. That this explanation is not correct is seen in Fig. 3. In panel *a*, the solid line shows the absolute spectrum at the end of a reductive titrate in the presence of egg homogenate and 1.2 mM $K_3Fe(CN)_6$ and being held at 460 mV for 1 h before the reduction. The short dashed line shows the spectrum taken 140 min after the first spectrum during which time the voltage of the medium was held at 100 mV. The long dashed line in the lower part of panel *a* shows the difference spectrum for the 140 min holding period. There was no decrease in amount of the predominant species with a Soret peak in absorbance near 428 nm. In panel *b*, the solid line shows a slow rise in the magnitude of the second derivative of absorbance vs. wavelength at 428 nm during a holding period of 140 min and the dashed line shows a slow decrease in the second derivative centered at 446 nm. Therefore, the 428 species appears to be stable.

In the absence of egg homogenate, 1.2 mM $K_3Fe(CN)_6$, or when exposure to high voltage is omitted, the predominant species of cytochrome a_3 seen initially is one that absorbs near 446 nm (panel *c*, solid line). However, upon holding at 130 mV, the 446 nm species slowly disappears (dashed line, panel *d*) as the 428 nm species appears (solid line, panel *d*). The absolute spectrum at the end of this time (short dashed line, panel *c*) shows a shift in absorbance from ~446 to 428 nm. The shift is especially clear in the difference spectrum between the start and end of the holding period (long dashed line, panel *c*). The same slow conversion of 446 nm species to 428 nm species is seen in panels *e* and *f* for a reductive titration in the presence of egg homogenate but absence of 1.2 mM $K_3Fe(CN)_6$ and exposure to high voltage. The role of the added egg homogenate, holding at high voltage and higher concentration of $K_3Fe(CN)_6$, therefore, is to facilitate the conversion of the 446-nm

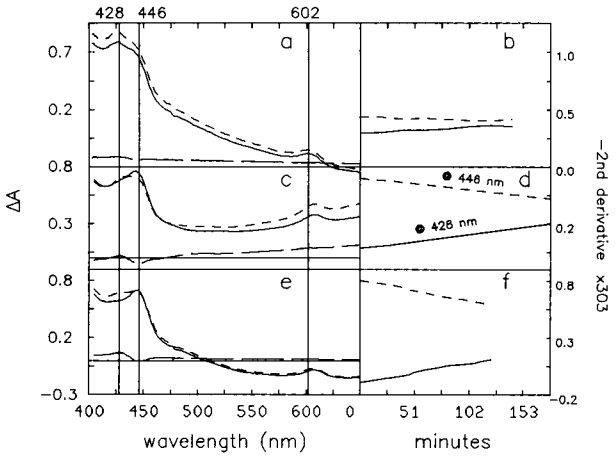

FIGURE 3 (*a*) Solid line shows the absolute spectrum obtained at the end of a reductive titration carried out as described in the legend to Fig. 1 *a*. After holding the preparation for 40 min at 100 mV, another absolute spectrum was taken (*short dashed line*). Long dashed line shows the difference spectrum obtained from these two absolute spectra. (*b*) Stability of the magnitudes of the second derivatives at 446 nm (*dashed line*) and at 428 nm (*solid line*). (*c*) Absolute spectrum (*solid line*) obtained at the end of a reductive titration conducted as described in Fig. 1 *b*. After holding the preparation at 140 mV for 3 h, another absolute spectrum was taken (*short dashed line*). The difference spectrum obtained from these two absolute spectra (*long dashed line*) shows the shift of the Soret peak from 446 towards 428 nm. The same slow conversion is shown by the second derivatives at 446 and 428 nm (*d*). (*e*) Absolute spectrum (*solid line*) obtained at the end of a reductive titration conducted as described in Fig. 1 *b*, except for the fact that egg homogenate was present. After holding at 95 mV for 2 h, the absolute spectrum was taken again (*short dashed line*). The difference spectrum obtained from these two absolute spectra (*long dashed line*) shows the shift of the Soret peak from 446 to 428 nm as do the magnitudes of the second derivatives at these wavelengths shown in *f*. Vertical lines are drawn at 428, 446, and 602 nm.

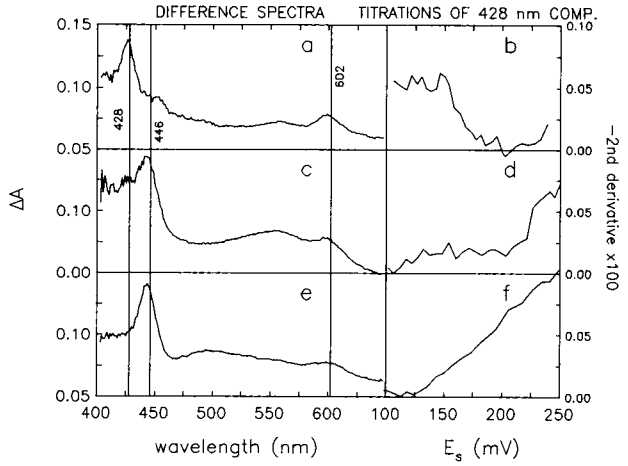

FIGURE 4 In these experiments, cytochrome aa_3 was incorporated into the membranes of asolectin proteoliposomes using the cholate dialysis technique of Hinkle et al. (1972) as described by Wrigglesworth et al. (1987). The procedure used for the experiments depicted in *a* and *b* was as described in Fig. 1 *a* using a 1-h holding period at 450 mV but omitting to add egg homogenate. (*b*) Titration of the second derivative at 428 nm and *a* shows the difference spectrum (146–200 mV). (*d*) Titration of the second derivative at 428 nm in an experiment where additions of egg homogenate and additional $K_3Fe(CN)_6$ were omitted as well as the preexposure to high voltage. (*c*) The difference spectrum obtained (98–198 mV). In the experiment shown in *e* and *f*, conditions were as described for *c* and *d* above except that 1.2 mM $K_3Fe(CN)_6$ was present. The difference spectrum shown in *e* was for 98–157 mV.

species to the 428-nm species rather than to impose a different stable reduction state.

To test the hypothesis that the egg homogenate was providing a lipoprotein environment for the enzyme, cytochrome oxidase was incorporated into proteoliposomes (Hinkle et al., 1972; Wrigglesworth et al., 1987) and the egg homogenate was not provided. The cytochrome oxidase vesicles formed in this way, displayed a respiratory control index of ~16, and were capable of forming a $\Delta\Psi$ and a ΔpH upon respiration supported by ascorbate, TMPD and cytochrome *c*. Fig. 4 *b* shows the titration of the second derivative at 428 nm of the cytochrome oxidase vesicles in the absence of egg homogenate. Panel *a* shows the difference spectrum (146–200 mV) with a Soret peak at ~428 nm and an α peak at ~602 nm in this titration. Panel *d* shows the titration of the second derivative at 428 nm for cytochrome oxidase vesicles not previously held at high voltage and in the presence of only 0.2 mM $K_3Fe(CN)_6$. The decrease in magnitude of the second derivative in going from 250 mV to lower voltages is due to the inverse titration of the cytochrome a_3, high potential form. The important thing to note is the absence of a rise in the voltage region, 200 to 150 mV. This plus the difference spectrum (98–198 mV) in panel *c* shows the absence of the 428 nm species. Panels *e* and *f* show the results of a titration of the cytochrome oxidase vesicles in the presence of 1.2 mM $K_3Fe(CN)_6$, but not preheld at high voltage. The absence of the 428 nm species is also seen under these conditions. Placing the enzyme in a proteoliposome membrane, eliminates the need for egg homogenate to form the a_{3L} (428/602) species, but the requirements for ~1 mM $K_3Fe(CN)_6$ and initial exposure to high voltage still remain.

Both a_{3L} (428/602) and a_{3L} (446) form a (different) CO-complex

To minimize the formation of a_{3L} (428/602), a reductive titration was performed without establishing any of the three conditions described above. After verifying that there was no evidence of a_{3L} (428/602) by use of second

derivatives, and difference spectra, the argon atmosphere was replaed by CO, and spectra were taken every 10 min for 60 min. Fig. 5 *b* shows the time course for the formation of the Soret peak of this CO complex at 433 nm (solid line) and the disappearance of the nonliganded a_{3L} (446) Soret peak at 446 nm (dashed line). Fig. 5 *a* shows the difference spectrum for the 60 min exposure to CO. The characteristic Soret peak for CO-liganded cytochrome a_3 normally seen near 433 nm has been displaced to 431 nm by the deep trough at 446 nm. The α peak for the CO-liganded enzyme at 593 is seen.

When all three conditions were set for the formation of a_{3L} (428/602), and the second derivatives and difference spectra confirmed its presence, the argon atmosphere was switched to CO and spectra were taken every 10 min for 60 min. Fig. 5 *d* shows the formation of the Soret peak at 433 nm (a_{3L}^{2+}-CO) (solid line). It is seen that the complex forms more slowly from the a_{3L} (428/602) form than from the a_{3L} (446) form (cf. Fig. 6 *b*). Furthermore, both the second derivative at 446 nm (Fig. 6 *d*) and the difference spectrum (Fig. 6 *c*) show that the formation of a_3^{2+} (428)-CO was not accompanied by a major disappearance of a Soret peak at 446 nm as was seen in panels *a* and *b*.

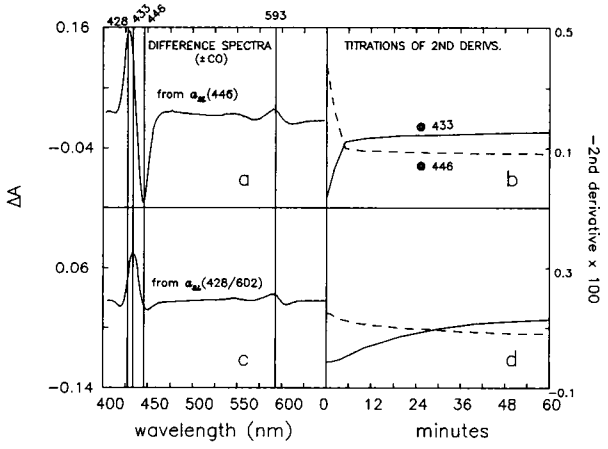

FIGURE 5 A reductive titration down to 150 mV was performed as described in Fig. 1 *a*. After it was established using second derivatives at 428 and 446 nm and by taking difference spectra, that a_{3L} (446) was formed rather than a_{3L} (428/602), the argon gas phase was replaced by CO and changes in the magnitudes of the second derivatives at 433 and 446 nm were followed at time points of 0, 2, 5, 10, 20, 30, 45, and 60 min (*b*). The difference spectrum obtained for the 60-min exposure to CO is shown in *a*. (*c* and *d*) Results obtained in an experiment where reduction was first performed using $Na_2S_2O_4$ as described in Methods (procedure b). (*d*) Changes in magnitude of the second derivatives at 433 nm (*solid line*) and at 446 nm (*dashed line*) at time points of 0, 1, 4, 10, 20, 30, 40, 50, and 60 min, during exposure to CO. (*c*) Difference spectrum obtained over this 60-min exposure to CO.

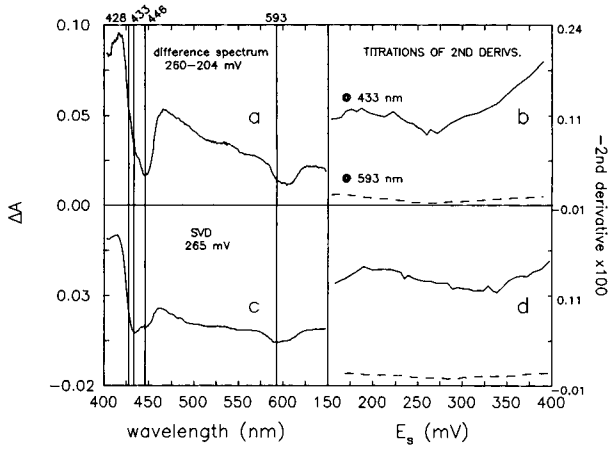

FIGURE 6 Electrical oxidation of the CO-liganded a_{3L} (428/602) species. The results of two separate experiments are shown. In one case the a_{3L} (428/602) species was formed in a reductive titration performed under conditions described in Fig. 1 *a*. After forming the CO complex by exposure to CO for 1 h, an oxidative titration was performed. The oxidation of a_{3L} (428/602) · CO is indicated by the declines in the second derivatives at 433 and 593 nm in the 200–270 mV region (*b*). The difference spectrum (260–204 mV) in *a* further documents this oxidation by the shoulders at 433 and 593 nm in troughs at 446 and 607 nm caused by the simultaneous oxidation of cytochrome *a*. In a separate experiment, a_{3L} (428/602) was formed by the $Na_2S_2O_4$ procedure (procedure b) and its CO complex was formed by a 1 h exposure to CO. The oxidation of a_{3L} (428/602) · CO is indicated by the declines in magnitudes for the second derivatives at 433 and 593 nm in the 200–350 mV range (*d*) and by the SVD-deduced difference spectrum for a transition with E_m = 265 mV (*c*). Distinct troughs are seen at 433 and 593 nm.

Midpoint potentials of CO complexes of a_{3L} (428/602) and a_{3L} (446)

In our earlier work with the pure enzyme (Hendler et al., 1986), the a_{3L} (428/602) species was the predominant form seen. In reductive titrations we reported that the E_m of the predominant CO-liganded form was ~200 mV. This conclusion was corroborated in experiments with intact beef heart mitochondria where the second derivative of the α peak of the CO complex near 593 nm was used as well as analyses by SVD (Reddy et al., 1986). An extension of this earlier work reported in the current communication is the redetermination of the E_m in oxidative titrations. The results of two such titrations are presented in Fig. 6. The oxidation of the CO complex made from a_{3L} (428/602) is indicated in panels *b* ande *d*. The solid lines show that the magnitudes of the second derivatives at 433 nm for two oxidative titrations decrease in the range of 200 to ~270 mV in panel *b* and to ~350 mV in panel *d*. This is to be contrasted with the behavior

of the 428-nm Soret peak in the absence of CO, which showed a continued rise in this voltage region in both reductive titrations (Fig. 1; see also Hendler et al., 1986) and oxidative titrations (Figs. 8 and 11). The second derivative at 593 nm, although of much smaller magnitude, also shows a drop in these voltage regions (dashed lines, Fig. 7, panels *b* and *d*). In the voltage range of 200–400 mV, the oxidation of cytochrome *a* leads to troughs at ~446 and 606 nm and a peak at ~420 nm. The formation of the reduced form of high potential cytochrome a_3 in this voltage range leads to a rise in the Soret peak at 428 nm. The oxidation of a_{3L} (428) · CO in this voltage range will be seen as a shoulder at ~433 nm in the trough with a minimum at 446 nm and a maximum near 420 nm; and as a shoulder at ~593 nm in the trough formed at ~606 nm. These features are clearly evident in the difference spectrum (260–204 mV) shown in panel *a* (Fig. 6) for one of the two titrations. The disappearance of the characteristic Soret and α absorbances at 433 and 593 nm, respectively, are more evident in the SVD-deduced difference spectrum for a transition at 265 mV in a separate titration (panel *c*).

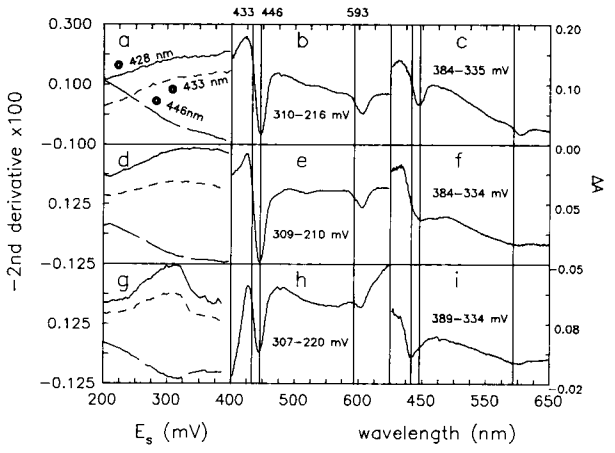

FIGURE 7 Electrical oxidation of the CO-liganded a_{3L} (446) species. Panels *a–c* were obtained from an oxidative titration of a_{3L} (446) performed in the absence of CO. The a_{3L} (446) species was formed in a reductive titration in which egg homogenate, extra $K_3Fe(CN)_6$ and preexposure to high voltage were eliminated. (*a*) The reciprocal relationship between the peaks at 428 and 446 nm in the voltage range 200–400 mV. The second derivative at 433 nm reflects the rise in the nearby feature at 428 nm. (*b*) Oxidation of cytochrome *a* in the 216–310 mV range as marked by the troughs at 446 and 607 nm and the peak near 420 nm. The increase in peak height at 428 nm is seen only as a shoulder on the deep trough at 446 nm. The important point to notice in this panel as well as panel *c* showing the difference spectrum 384–335 mV is the absence of any shoulders at 433 and 593 nm in the troughs at 446 and 607 nm. In contrast to the data shown in *a–c*, the remaining panels do show evidence of oxidation of the CO complex of a_{3L} (446). Panel *d* shows that instead of rising throughout the oxidation range, the second derivative at 433 nm (*dashed line*) shows a decrease in the range above 300 mV. There was no decrease in the range 200–300 mV where the CO complex of a_{3L} (428/602) was seen to be oxidized. The lack of oxidation of the CO complex of a_{3L} (446) in the 200–300 mV range is further shown by the difference spectrum (309–210 mV) in *e*. Panel *f* corroborates the oxidation of the CO complex indicated by the drop in magnitude of the second derivative at 433 in *a*. Distinct shoulders at 433 and 592 nm are seen in the troughs at 446 and 607 nm. The clearest demonstration of the oxidation of a_{3L} (446) · CO in the voltage range above 300 mV is seen in *g* and *i*. The decline in magnitude of the second derivative at 433 nm was so marked (*short dashed line; g*) that the second derivative at 428 nm reflected this change (*solid line; g*). Panel *i* clearly shows the trough at 433 nm as well as a strong shoulder at 593 nm. Panel *h* shows the usual seesaw relationship between the Soret peaks at 428 and 446 nm but no evidence of oxidation of a_{3L} (446) · CO in this region.

The oxidation of the a_{3L} (446) · CO complex was much more difficult to detect. In addition to the fact that, as in the case for the oxidation of the a_{3L} (428) · CO complex, the oxidized spectrum is seen as shoulders on troughs occurring as a result of cytochrome *a* oxidation, it was found that CO quite often induced the formation of an appreciable amount of a_{3L} (428) · CO from the a_{3L} (446) precursor, resulting in oxidation in the 200–260 mV region. In several experiments, however, a clear-cut oxidation in the voltage range of ~325 to 375 mV was seen. Fig. 7, *a–c*, were obtained from an oxidation in the absence of CO and are used for references in evaluating the other panels obtained in two experiments during which the a_{3L} (446) · CO complex was oxidized. In all cases, in the voltage range 200–400 mV, the second derivative at 428 nm is expected to rise with voltage due to the formation of the reduced form of high potential cytochrome a_3 (Hendler and Sidhu, 1988). This is seen in the solid line of panel *a*. Also shown in panel a is the continual rise in the second derivative at 433 nm (short dashed line). This is because the second derivative at 433 nm responds to the change in magnitude of the nearby Soret with its peak at ~428 nm. The oxidation of cytochrome *a* is documented by the fall in the second derivative at 446 nm (long dashed line). The lack of any sign of oxidation of a species absorbing at 433 nm seen in panel *a* is supported by the difference spectra in the range 216–310 mV (panel *b*) and 335–384 mV (panel *c*). There is no sign of a shoulder at 433 nm in the trough at 446 m nor at 593 nm in the trough at 606 nm. Therefore, the appearance of shoulders at 433 nm and at 593 nm in oxidative experiments in the presence of CO can be taken as evidence for the oxidation of the cytochrome a_3-CO liganded complex. In panel *d*, there is no sign of oxidation of the 433 nm peak of the CO complex in the 200–300 mV range as was seen in the case of the a_{3L} (428) · CO complex. The difference spectrum in the range 210–309 mV (panel *e*) also shows no sign of oxidation. The second derivative at 433 nm (short dashed line, panel *d*) does show a decrease, however, above 300 mV. Panel *f* shows

that for the difference spectrum in the range of 334–384 mV, a shoulder at 433 nm is seen and that the α region absorbance depression does extend into the 593-nm range. A separate experiment shown in panels *g–i* provides a much clearer case for oxidation of the Soret at 433 nm in the voltage region, 325–400 mV. Panel *g* shows the titration of the second derivative at 435 nm. Panel *h* (307–220 mV) shows the usual seesaw relationship (Hendler et al., 1986) for the oxidation of cytochrome *a* (trough at 446 nm) and reduction of high potential cytochrome a_3 (peak near 428 nm). The oxidation of a_{3L} (446) · CO is clearly seen in panel *i* (334–389 mV) with the trough at 433 nm and a prominent shoulder at 593 nm.

The titrations shown in Figs. 6 and 7 in which both forms of a_{3L}-CO complex were oxidized below 400 mV are at odds with the commonly held belief that $K_3Fe(CN)_6$ cannot oxidize CO-liganded cytochrome a_3 (Wikström et al., 1981; Horie and Morrison, 1963; Wilson and Leigh, 1974; Ellis et al., 1986; Wever et al., 1974).

To subject this question to a more direct test we performed chemical oxidations of both species, using $K_3Fe(CN)_6$ as the oxidant. a_{3L} (428/602) was made in a reductive titration using cytochrome aa_3 incorporated into liposomal vesicles. The CO complex was made during a subsequent 70 min exposure to CO. Fig. 8 shows the results obtained in a chemical oxidative titration of this a_{3L} (428) · CO. Panel *a* shows the decrease in the second derivative at 433 nm in the voltage range, 200 to ~275 mV. Panel *b* shows the decrease in the second derivative at 593 mV. Both curves, although noisy, indicate an E_m near 225 mV. Panel *c* shows the difference spectrum 263–194 mV. The titration of the Soret peak at 433 nm and the α peak at 593 nm is clearly shown. SVD analysis found two titrating species one with E_m = 186 mV (panel *d*) and one with E_m = 248 mV (panel *e*). Fig. 9 shows the results obtained when a_{3L} (446) · CO was titrated. Both the second derivative at 433 nm (panel *a*) and at 593 nm (panel *b*) show a rise in the voltage range 225–300 mV and a decrease (oxidation) in the range 300–375 mV. The difference spectrum (358–307 mV) in panel *c* and the SVD derived difference spectrum for a component with E_m = 321 mV in panel *d* both document the oxidation of a_{3L} (446) · CO in the region 300–370 mV. Both forms of CO-liganded cytochrome a_3 are oxidized at room temperature by $K_3Fe(CN)_6$.

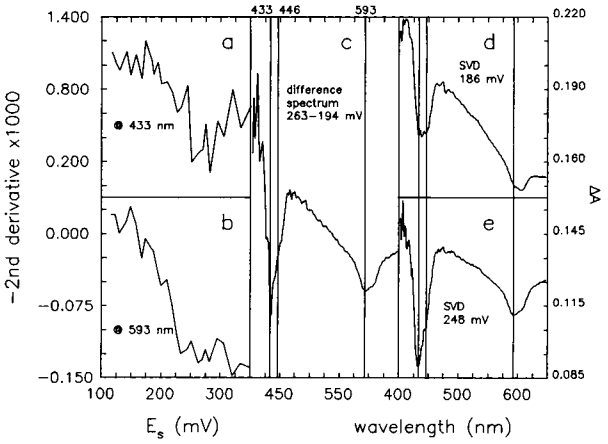

FIGURE 8 Chemical oxidation of the CO-ligand a_{3L} (428/602) species using $K_3Fe(CN)_6$ as oxidant. a_{3L} (428/602) was made during a reductive titration using cytochrome aa_3 incorporated into liposomal vesicles as described in the legend to Fig. 5. The CO complex was made during a 70-min exposure to CO. Oxidation was carried out using microliter additions of 1 M $K_3Fe(CN)_6$. (*a* and *b*) Oxidation of the CO complex as indicated by the decreases in the magnitude of the second derivatives at 433 and 593 nm. The oxidation of the CO comples is shown in the difference spectrum (263–194 mV) in *C* with troughs at 433 and 593 nm. The ΔA range in *c* extends from 0.1 to 0.25 U. SVD analysis saw two oxidative transitions, one at 186 mV (*d*) and one at 248 mV (*e*). Both show pronounced depressions at 433 and 593 nm.

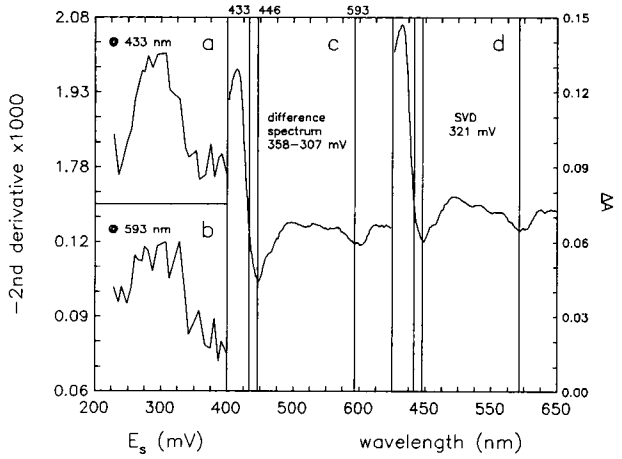

FIGURE 9 Chemical oxidation of the CO-ligand a_{3L} (446) species using $K_3Fe(CN)_6$ as oxidant. a_{3L} (446) was made during a reductive titration of the pure enzyme under conditions described in Fig. 1 *b*. The CO complex was made during a 40-min exposure to CO. The difference spectrum showed a deep trough at 446 nm and a sharp peak near 433 nm as shown in Fig. 6. Using $K_3Fe(CN)_6$ as the oxidant resulted in no decrease for either the second derivative at 433 or 593 nm in the voltage region 200–300 mV (*a* and *b*), but marked decrease were seen in the region 300–375 mV. The oxidation of the CO complex is seen in the difference spectrum (358–307 mV) in *c* by the pronounced shoulders at 433 and 593 nm in the troughs at 446 and 607 nm caused by the oxidation of cyrochrome *a*. The oxidation of cytochrome *a* also causes a peak near 420 nm. The SVD-deduced spectrum for a transition with E_m = 321 mV also shows the depressions at 433 and 593 nm caused by the oxidation of a_{3L} (446) · CO.

Oxidation of a_{3L}^{2+} (428) and a_{3L}^{2+} (446)

In our earlier publication we described a major Soret peak at ~428 nm with a prominent shoulder at ~446 nm when reductive titrations were performed in the presence of egg homogenate. In Fig. 2, the 446-nm absorbance is sufficiently prominent to be discernible as a separate peak. The reversibility of this behavior, however, was not observed when an oxidative titration was performed. The difference spectrum obtained upon oxidation showed a major trough at ~446 nm (not at 428 nm) and sometimes a shoulder at ~428 nm in the trough. This was one of the reasons why we considered that the a_{3L} (428/602) form might be a labile species, which is generated by reduction, and which decays before the oxidation of it could be accomplished. In Fig. 3 of this paper, we present evidence that a_{3L} (428/602) is stable but that a_{3L} (446) is unstable and that it is continuously converting into the 428-nm form. Therefore, a reasonable explanation for the difficulty in demonstrating reversibility in the titration of the a_{3L} (428/602) species is the following. Even in the presence of egg homogenate, there is always a certain fraction of a_{3L} in the 446-nm form. Upon oxidation, in addition to the decrease of the a_{3L}^{2+} (428/602) form by its oxidation, there is a continual regeneration of the a_{3L}^{2+} (428/602) species from the a_{3L} (446) which is present. That the generation of a_{3L}^{2+} (428/602) from a_{3L}^{2+} (446) continues to occur during the oxidative phase is seen in Fig. 11, which will be discussed shortly. Whether or not a distinct trough at 428 nm is seen during an oxidation depends on the balance between these two processes. That a_{3L}^{2+} (428/602) is indeed oxidized, and at the same apparent E_m as seen for its reduction is shown in Fig. 10. The characteristic α absorbance at ~602 nm shows oxidation in the 160–200 mV range (panel *b*). There is a concomitant oxidation of the 428-nm feature (panel *a*). After reaching a minimum near 200 mV, the second derivative at 428 nm starts its rise, which will continue up to >400 mV. The oxidation of the a_{3L}^{2+} (428/602) species in the voltage range 160–200 mV is shown by the difference spectrum in panel *c*. SVD analysis produced the difference spectrum shown in panel *d* for a transition with E_m = 178 mV. It is evident in this figure as well as in Fig. 2 (panels *a* and *b*) and Fig. 4 (panel *a*) that the ratio of the absorbances of the reduced Soret and α peaks is much smaller for the a_{3L} (428/602) species than for cytochromes in general, including cytochrome oxidase. It should also be stressed that the titration shown in Fig. 10 is one of the most successful for seeing the 428- and 602-nm features clearly stand out during the oxidation. In most cases, the 428-nm feature is seen only as a shoulder in a trough with a minimum at 446 nm. The 602-nm feature, however, is usually seen as a trough in an oxidative titration.

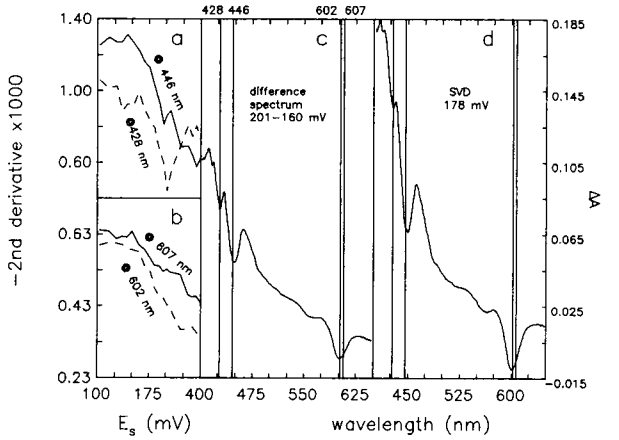

FIGURE 10 a_{3L} (428/602) was made using $Na_2S_2O_4$ as described in Methods (procedure b). The oxidation of a_{3L} (428/602) is shown by the decreases in magnitude of the second derivatives at 428 nm (*a*) and at 602 (*b*). The difference spectrum in *c* (201–160 mV) and the SVD-deduced difference spectrum in *d* both show the oxidation of the Soret peak at 428 nm and the α peak at 602 nm.

When none of the conditions for rapidly forming the a_{3L} (428/602) species is met, only the a_{3L} (446) species is seen, and an oxidative titration produces the results shown in Fig. 11. Panel *a* shows the disappearance of the second derivative at 446 nm with a particular steepness in the 120–185 mV region, but continuing throughout the whole range shown. It can be seen that the 428-nm feature rises throughout the whole region. The changes occurring near 100 mV reflect the continuing conversion of a_{3L} (446) to a_{3L} (428) discussed above and shown in Fig. 3. The lack of a contribution due to the oxidation of cytochrome *a* is shown by the absence of a trough at 606 nm in the difference spectrum occurring during the titration in this range (panels *c* and *e*). The changes occurring with an E_m of 200 mV (panels *d* and *f*) show the oxidation of a_{3L} (446). In reductive titrations the rise in the peak at ~446 nm also occurs with an E_m of ~200 mV (Table 3). The oxidation of cytochyrome *a* with its α feature at 607 nm and E_m near 260 mV is shown by the behavior of the second derivative at 607 nm in the voltage range above 200 mV (panel *b*). It is also seen that the feature at 602 nm shows no drop in the voltage range 120–185 mV, where the second derivative at 446 nm showed its steepest drop (panel *a*). This means that either there is no α feature at 602 nm for a_{3L}^{2+} (446) or that it is of sufficiently lesser magnitude compared to the a_{3L} (428) species that, although it is being titrated away by oxidation, it is more than compensated for by generation of the

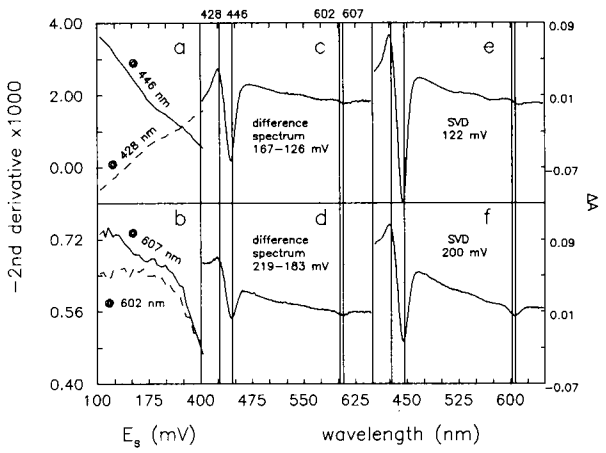

FIGURE 11 a_3 (446) was made using the $Na_2S_2O_4$ reduction technique as described in Methods (procedure b). The oxidation of a_{3L} (446) is indicated by the decrease in magnitude of the second derivative at 446 nm (*a*) with a particular steepness in the 120–185 mV region. The second derivative at 602 nm shows no decrease in this region (*b*). The difference spectrum in *c* and the SVD-deduced difference spectrum in *e* both show distinct troughs at 446 nm, a small change in the 600–610 nm region and a rise at 428 nm signifying the continuing formation of a_{3L} (428/602). The direct difference spectrum in *a* and the SVD-deduced spectrum in *f* show changes indicating the oxidation of both a_{3L} (446) and cytochrome *a* with its α peak at 607 nm.

a_{3L} (428/602) species. Panel *c* shows the difference spectrum for the voltage range of the steepest drop in the magnitude of the second derivative at 446 nm. There is a sharp trough at 446 nm and a peak at 428 nm. The α region shows no distinct features. Panel *e* shows one of the two difference spectra deduced by SVD for the titration through this voltage range. The E_m was seen at 122 mV. Panel *f* shows a second transition seen by SVD. In addition to the general similarity to the spectra shown in panels *c* and *e*, a prominent α trough at ~606 nm is seen, indicating that some of the titration of cytochrome *a* is included in this difference spectrum. Panel *d* is a difference spectrum for the 219–183 mV range, and it is quite similar to the spectrum shown in panel *f*.

E_m values for a_{3L} (428/602) and a_{3L} (446) and their CO-liganded forms

A summary of the fitted E_m values for the two low-potential forms of cytochrome a_3 based mainly on the current work, but with additional information, where appropriate, from earlier studies is shown in Tables 1–3. We have consistently found that $n = 2$ provides much better fits than $n = 1$ and all of the values shown in these summary tables were obtained using $n = 2$. Table 1 shows results obtained in the absence of CO. The table is divided into two parts. In part 1, all three conditions (egg homogenate or incorporation into liposomes, initial holding at high voltage, and ~1 mM $K_3Fe[CN]_6$ present) for the formation of the a_{3L} (428/602) species were met. Part 2 describes results obtained when the three conditions were not met and therefore the a_{3L} (446) species predominated (or was exclusively present). In the absence of CO, the E_m of the a_{3L} (428/602) species was found to be close to 180 mV. This followed from the second derivatives at both 428 and 602 nm, and also from SVD analysis, and both for oxidative and reductive titrations. In an earlier study with the pure enzyme, the second derivative at 428 nm produced an E_m of 173 mV. Although the a_{3L} (428/602) species predominated when all three conditions were met, there was always a certain amount of a_{3L} [446] present). Table 1 shows that analyses based on the second derivative at 446 nm found the E_m of this species to be 204 mV. In the earlier study with the pure enzyme, the second derivative at 446 nm produced an E_m of 202 mV. In the same earlier study, SVD must have been influenced by this species insofar as SVD produced an E_m at 196 mV. A second derivative analysis at 604 nm produced an E_m at 193 mV and in a study with intact beef heart mitochondria, SVD produced an E_m of 206 mV and the second derivative at 604 nm yielded at E_m at 196 mV.

When conditions for forming the a_{3L} (446) species rather than the a_{3L} (428/602) species were used, the second derivative at 446 nm showed two titrations, one at 206 mV and one at 148 mV (Table 1). SVD analysis showed two titrations; one at 183 mV and the other at 133 mV. In the earlier studies, only the conditions for forming the a_{3L} (428/602) species were used. A summary of these E_m values obtained in the absence of CO is recapitulated in Table 3.

Titrations performed under a CO atmosphere are described in Table 2. Under conditions favoring the a_{3L} (428/602) species, the results of the current investigations show an E_m near 230 mV. This is true using second derivative at 433 nm and at 593 nm and with SVD analysis, and both for reductive and oxidative titrations. In the earlier paper using the pure enzyme, an E_m value close to 200 mV was seen in two reductive titrations. The latter value was also seen in a study using intact mitochondria. In the earlier study using the pure enzyme, as well as in the current studies, a second (minor) transition was seen in reductive titrations with an E_m near 120 mV. For the major CO complex made from the a_{3L} (428/602) species, the presence of CO raised the E_m of the titration ~60 mV in the current studies and ~30 mV if both the current and earlier studies are considered (Table 3). For a reaction with $n = 2$ this requires that the affinity of CO for the reduced species be 10–100 times greater than for the oxidized species.

TABLE 1 Summary of E_m's (−CO)

This paper			Earlier papers: Pure enzyme*	Earlier papers: Mitochondria‡
		Second derivative analysis		
1. Under conditions for forming a_{3L} (428/602)				
At 428 nm				
Reductions	164 ± 6 (8)		173 ± 5 (5)	—
Oxidations	189 ± 5 (2)		—	—
All	169 ± 6 (10)			
At 602 nm				
Reductions	170 ± 5 (8)			
Oxidations	187 ± 6 (4)			
All	176 ± 4 (12)		193 ± 5§ (13)	196 ± 8§ (12)
At 446 nm				
Reductions	208 ± 2.4 (7)		212 ± 7 (8)	—
Oxidations	196 ± 1.6 (4)		187 ± 9 (5)	—
All	204 ± 3 (11)		202 ± 6 (13)	
		SVD analysis		
Reductions	185 ± 7 (4)		202 ± 2 (6)	207 ± 7 (7)
Oxidations	175 ± 8 (3)		189 ± 6 (3)	203 ± 9 (3)
All	181 ± 5 (7)		196 ± 3 (9)	206 ± 5 (10)
		Second derivative analysis		
2. Under conditions for forming a_{3L} (446)				
At 446 nm				
Reductions	210 ± 4 (7)	156 ± 3 (7)	—	—
Oxidations	198 ± 16 (3)	130 ± 7 (3)	—	—
All	206 ± 5 (10)	148 ± 5 (10)	—	—
		SVD analysis		
Reductions	188 ± 5 (2)	141 ± 3 (2)	—	—
Oxidations	178 ± 22 (2)	124 ± 2 (2)		
All	183 ± 10 (4)	133 ± 5 (4)	—	—

Data are shown as average ± SEM for the number of determinations shown in parentheses. *Hendler et al., 1986. ‡Reddy et al., 1986. §The α peak was at 602 nm, but the second derivative analysis was at 604 nm in order to follow the titrations of either or both of the α peaks for cytochrome a (606–607 nm) and of cytochrome a_3 (602 nm).

The E_m of the a_{3L} (446) species is seen at near 200 mV both under conditions favoring the a_{3L} (428/602) species and under conditions which repress its formation (Table 1). In the latter case, however, an additional transition with an E_m near 140 mV is seen. Titrations performed under a CO atmosphere when the a_{3L} (446) species was the only one seen before switching to CO produced an E_m of 335 mV (Table 2, Part 2). It should be noted that these were all oxidative titrations (both electrical and chemical). To minimize the tendency to form the a_{3L} (428/602) species, there was no initial raising of the voltage of the solution above the usual ~270 mV starting voltage in the presence of the enzyme and redox mediators. At this voltage the tendency to form the a_{3L} (446) · CO complex proved to be so high that an additional growth of the Soret at 433 nm and α peaks at 593 nm upon a reductive titration was not seen. The very high tendency for CO to bind to a_{3L} (446) at these voltages can be seen in the relative E_ms of the free and CO liganded species. The E_m of the CO-liganded form (i.e., 335 mV) is ~120 mV higher than that of the 200-mV form of the unliganded species and ~180 mV above that of the 140-mV species (Table 3). For $n = 2$ redox transitions this implies a 10^4–10^6 greater binding affinity of CO for the ferrous form of a_{3L} (446) than for the ferric form. Therefore under a CO atmosphere with a solution voltage near 270 mV, the a_{3L} (446) species is "pulled" from the ferric to the ferrous and finally the CO-liganded ferrous form.

An overall summary of all of the E_ms in the presence and absence of CO is presented in Table 3.

TABLE 2 **Summary of E_m's (+CO)**

	This paper		Earlier papers			
			Pure enzyme*		Mitochondria‡	
Second derivative analysis						
1. Formation of CO complex from a_{3L} (428/602)						
At 433 nm						
Reductions	227 ± 12 (6)	105 ± 3 (2)	202 ± 10 (2)	113 ± 6 (2)	—	
Oxidations	228 ± 13 (5)		—		—	
All	228 ± 8 (11)					
At 593						
Reductions	222 ± 14 (7)	138 ± 10 (3)	199 ± 8 (2)	116 ± 7 (2)	198 ± 4 (3)	158 ± 5 (3)
Oxidations	222 ± 5 (5)		—		—	
All	222 ± 8 (12)					
SVD analysis						
Reductions	208 ± 17 (3)		208 ± 2 (2)	105 ± 2 (2)	195 ± 8 (3)	136 ± 13 (3)
Oxidations	246 ± 7 (4)		—		—	
All	230 ± 11 (7)					
Second derivative analysis						
2. Formation of CO complex from a_{3L} (446)						
At 433 nm						
Reductions	§					
Oxidations	337 ± 12 (3)					
At 593 nm						
Reductions	§					
Oxidations	336 ± 12 (2)					
SVD analysis						
Reductions	§					
Oxidations	331 ± 10 (2)					

*Hendler et al., 1986. ‡Reddy et al., 1986. §Because of the strong tendency of a_{3L} (446) to bind CO, reductive titrations in the presence of CO could not be performed, as explained in the text.

DISCUSSION

Relevance of present findings to past studies with cytochrome *c* oxidase

About 10 years ago, Nicholls and Hildebrandt (1978) provided evidence that, upon reduction of isolated resting cytochrome oxidase, cytochrome a_3 undergoes a spin state transition with an accompanying red shift in its Soret position from ~418 to ~433 nm. At the same time a small blue shift occurred for the α peak. The reduction of cytochrome a_3 was accompanied by a decline in the percentage reduction of cytochrome a. Similar spin state changes were seen upon reduction in mitochondria and submitochondrial particles. Nicholls and Hildebrandt speculated that, although with the isolated enzyme the low-spin form of cytochrome a_3 in the partially reduced enzyme is transient, the same species could be stabilized in a membrane-bound form such as would occur in situ. More recently Nicholls and Wrigglesworth (1989) attributed the initial reduction site in the resting enzyme to Cu_B. They believe that the reduction of Cu_B is the trigger which starts the transformation of high-spin ferric cytochrome a_3 to the low-spin form.

Wrigglesworth et al. (1988) have correlated the apparent spin shift transition for cytochrome a_3 during turnover of the initially resting enzyme with the generation of the fast-reacting form of cytochrome a_3, with respect to reduction by dithionite or ascorbate/TMPD or CN^- binding. A further indication of the conversion of the resting enzyme to a catalytically more active form is the disappearance of the $g = 12$ signal used by Baker et al. (1987) as an indicator of the slow reactive species of cytochrome a_3. The shift of the Soret peat from a position of ~420 nm in the resting enzyme to ~428 nm, and the α peak from ~605 to near 602 nm accompanying a transformation of the enzyme from a sluggish to a more reactive

TABLE 3 Total picture E_m's

Second derivative	−CO	+CO	This paper	Earlier papers: Pure aa_3*	Earlier papers: Mitochondria‡
	mV	*mV*			
a_{3L} (428/602)					
Soret peak (*nm*)					
428	169		X		
428	173			X	
433		228	X		
433		202		X	
α Peak (*nm*)					
602	176		X		
593		222	X		
593		199		X	
593		198			X
SVD analysis	181		X		
	196			X	
		230	X		
		208		X	
		195			X
AV					
This paper	175 ± 3 (3)	227 ± 2 (3)			
All three papers	179 ± 5 (5)	210 ± 5 (8)			
ΔE_m(+CO −CO)					
This paper			52 (i.e., 227–175 mV)		
All three papers			21 (i.e., 210–179 mV)		
a_{3L} (446)					
Soret Peak (*nm*)					
446§	204		X		
446 (h)	206		X		
446 (l)	148		X		
446§ (h)	202			X	
@433		337	X		
@593		336	X		
SVD analysis					
(h)	183		X		
(l)	133		X		
		331	X		
AV (h)	199 ± 5 (4)				
(l)	140 ± 8 (2)	335 ± 2 (3)			
ΔE_m(+CO −CO) (h) 136‖					
(l) 195¶					

*Hendler et al., 1986. ‡Reddy et al., 1986. §Present under conditions for making a_{3L} (428/602): (h) higher E_m component of a_{3L} (449); (l) lower E_m component of a_{3L} (446). ‖i.e., 335–199 mV. ¶i.e., 335–140 mV.

form was reported more than 30 years ago by Okunuki et al. (1957).

With these observations as background, it seems quite possible that the low-potential form of the enzyme with a Soret peak near 428 nm and an α peak near 602 nm which we describe here, and previously for the pure enzyme (Hendler and Sidhu, 1988) and for the enzyme in situ in mitochondria (Reddy et al., 1986), could be a stabilized form of the more reactive, low-spin species of the enzyme normally seen under turnover conditions. The results in the present paper suggest that this form of the enzyme would not be seen in potentiometric titrations as normally conducted. Instead, the high-spin form with a Soret peak near 446 nm and a very small α peak near 600 nm would be seen. The critical factors for forming the apparently low-spin species of reduced cytochrome a_3 (Soret peak ~428 nm and α peak ~602 nm) are: providing the enzyme with a lipoprotein environment (either adding egg homo-

genate or incorporating the enzyme in a liposome, or in situ), brief exposure of the enzyme to high voltage (~30 min at ~470 mV), and the presence of ~1 mM $K_3Fe(CN)_6$ during the reductive titration to ~100 mV. The latter requirement may be needed for adequate mediation between the Pt electrode and redox sites of the membrane-bound enzyme.

Redox transitions in the 100–400 mV range

In the current paper, we show that the low-voltage redox transition, which we previously described for the lipoprotein supplemented enzyme, at ~190 mV (Hendler et al., 1986), really consists of two species. One is the species with a reduced Soret peak ~428 and a prominent α peak near 602 nm and with an E_m of ~180 mV. The other has a reduced Soret peak ~446 nm, no prominent α peak, and an E_m ~200 mV. Previously, we described two other redox transitions in the intermediate voltage range, one at ~260 mV and the other at ~340 mV. The n values were 2 for all of the transitions except the one at ~340 mV which displayed an n = 1 value. Three redox transitions for bovine heart cytochrome *c* oxidase near 200, 260, and 340 mV have since been confirmed by Steffens and Buse (1988) and by Nicholls and Wrigglesworth (1988).

The identification of the two transitions which occur below 200 mV as being due to cytochrome a_3 is based on the demonstrated ability of both to form complexes with CO as described in this paper. Each of the two low-E_m forms has its own distinctive absorption spectrum and E_m value. The CO complexes formed from each show the expected reduced Soret peak near 433 nm and α peak near 593 nm. The E_m for the CO complex made from the 428-nm species of cytochrome a_3 is ~225 mV and the E_m for the CO complex made from the 446-nm species of cytochrome a_3 is ~335 mV. Both CO complexes are readily oxidized by $K_3Fe(CN)_6$ which has an E_m ~430 mV. This finding is in marked contrast to the commonly held view that in the presence of CO, the E_m of the reduced liganded form is so high that it locked into a reduced form that cannot be oxidized by $K_3Fe(CN)_6$ (Wikström et al., 1981; Horie Morrison, 1963; Wilson and Leigh, 1974; Ellis et al., 1986; Wever et al., 1977). Considering the apparent change in E_m of the CO complexes compared to the free forms of the enzyme (cf. Table 3), it is evident that the reduced form of the 428-nm species does bind CO more tightly than the oxidized form by ~10–100 to 1 and that the reduced form of the 446-nm species binds CO ~10,000 times more tightly than does its corresponding free form. But, considering the low E_ms of the free forms and the $n = 2$ nature of the redox changes, the elevated E_ms are still substantially below the E_m of $K_3Fe(CN)_6$. On the other hand, it has been well established that at cryogenic temperatures, CO-liganded cytochrome a_3 can be held in a reduced state as $K_3Fe(CN)_6$ is used to oxidize cytochrome *a*, thereby forming the mixed valence form of cytochrome oxidase (Clore et al., 1980; Wever et al., 1974; Chance et al., 1975).

The experiments with cytochrome oxidase present in a liposomal membrane, which removes the requirement for added egg homogenate to form the apparent low-spin species of cytochrome a_3, provide an explanation for the role of the lipid-rich egg supplement. Even in the presence of the lipoprotein environment, exposure to high voltage and the presence of ~1 mM $K_3Fe(CN)_6$ are still requirements for the immediate appearance of the 428-nm species of reduced cytochrome a_3. However, when none of the three requirements are met, and only the 446-nm species of reduced cytochrome a_3 is immediately seen upon reduction, there is a *slow* conversion of the 446-nm species to the 428/602 species. It seems that the apparent low-spin form is actually the more stable but that there is a kinetic barrier that must be overcome for the reduced form of the free enzyme to relax from the high-spin 446-nm species to the low-spin 428/602 species.

A caveat

The results of an intensive study of the redox behavior of mammalian cytochrome *c* oxidase using more powerful techniques of data acquisition and analysis reported in a series of papers from this laboratory and culminating in the present communication present a more detailed and accurate picture of this enzyme than was perceived on the basis of earlier techniques. It is not surprising that this very complicated enzyme with 13–14 metals per functional dimer (Einarsdóttir and Caughey, 1985), 9 or 10 of which are redox active, and which shows evidence of extensive redox cooperativity, displays more complex behavior than indicated by earlier work describing two equal $n = 1$ steps for the titration of the hemes. Although we were able to obtain consistent results for the E_ms of the lower-voltage forms of cytochrome a_3 described in this paper using second derivative analysis in both Soret and α peaks and by SVD analysis, and using both oxidative and reductive titrations, there are some uncertainties we must point out. In the voltage region where the low-E_m forms of free and CO-liganded cytochrome a_3 are titrating, many spectral changes are occurring. At low voltages there is a slow transformation of cytochrome a_{3L} (446) into cytochrome a_3 (428/602). In the region from 200 to 450 mV, the high-voltage form of cytochrome a_3 tends to become reduced, leading to a rise in absorbance at 428 nm, as the oxidation of the low-voltage forms causes a decrease in absorbances at 446 and 428 nm in the case of the unliganded species (Hendler and Sidhu, 1986) or at 433 nm in the case of the CO-liganded species.

None of these complications compromises the main findings reported in this paper that two forms of low-E_m cytochrome a_3 exist, that the 428/602 form is representative of a stable membrane-oriented form, that they both form CO complexes, that these complexes have different E_ms and that $K_3Fe(CN)_6$ is capable of oxidizing both complexes at room temperature. The reservation we wish to state is that although we have achieved consistency by a variety of analytical approaches in both oxidative and reductive experiments, the value for the E_ms we report may differ from the actual thermodynamic midpoint potentials by 15–20 mV. Additional, even more powerful techniques may have to be develooped before precise thermodynamic values of the E_ms can be stated with complete assurance.

The authors acknowledge the help of Dr. Frits Kamp for the preparation of tightly coupled cytochrome *c* oxidase liposomes, Dr. Winslow Caughey and Dr. Gary Yewey for the purified cytochrome *c* oxidase, Richard I. Shrager for the improved SVD procedure by which simultaneous fitting of all parameters to all titration eigenvectors with suitable weighting factors was done, and Dr. Hans V. Westerhoff for a careful reading of the manuscript and many helpful suggestions.

Received for publication 2 August 1989 and in final form 27 November 1989.

REFERENCES

Baker, G. M., M. Noguchi, and G. Palmer. 1987. The reaction of cytochrome oxidase with cyanide. *J. Biol. Chem.* 262:595–604.

Brunori, M., G. Antonini, F. Malatesta, P. Sarti, and M. T. Wilson. 1988. Structure and function of cytochrome oxidase: a second look. *Adv. Inorganic Biochem.* 7:93–153.

Carithers, R. P., and G. Palmer. 1981. Characterization of the potentiometric behavior of soluble cytochrome oxidase by magnetic circular dichroism. Evidence in support of heme-heme interaction. *J. Biol. Chem.* 256:7967–7976.

Chance, B., S. Saronio, and J. S. Leigh, Jr. 1975. Functional intermediates in the reaction of membrane-bound cytochrome oxidase with oxygen. *J. Biol. Chem.* 250:9226–9257.

Clore, G. M., L.-E. Andreasson, B. Karlsson, R. Aasa, and B. G. Malmström. 1980. Characterization of the intermediates in the reaction of mixed-valence-state soluble cytochrome oxidase with oxygen at low temperatures by optical and electron-paramagnetic resonance spectroscopy. *Biochem. J.* 185:155–167.

Einarsdóttir, D., and W. S. Caughey. 1985. Bovine heart cytochrome *c* oxidase preparation contain high affinity binding sites for magnesium, as well as for zinc, copper, and heme iron. *Biochem. Biophys. Res. Commun.* 129:840–847.

Ellis, W. R., H. Wang, D. F. Blair, H. B. Gray, and S. I. Chan. 1986. Spectroelectrochemical study of the cytochrome *a* site in carbon monoxide inhibited cytochrome *c* oxidase. *Biochemistry* 25:161–167.

Hartzell, C. R., and H. Beinert. 1976. Oxido-reductive titrations of cytochrome *c* oxidase followed by EPR spectroscopy. *Biochim. Biophys. Acta.* 423:323–338.

Hendler, R. W., and G. S. Sidhu. 1988. A new high potential redox transition for cytochrome aa_3. *Biophys. J.* 54:121–133.

Hendler, R. W., K. V. S. Reddy, R. I. Shrager, and W. S. Caughey. 1986. Analysis of the spectra and redoxy properties of pure cytochrome aa_3. *Biophys. J.* 49:717–729.

Hinkle, P. C., J. J. Kim, and E. Racker. 1972. Ion transport and respiratory control in vesicles formed from cytochrome oxidase and phospholipids. *J. Biol. Chem.* 247:1338–1339.

Horie, S., and M. Morrison. 1963. Cytochrome *c* oxidase components. *J. Biol. Chem.* 238:1855–1860.

Leigh, J. S., D. F. Wilson, C. S. Owens, and T. E. King. 1974. Heme-heme interaction in cytochrome x oxidase: the cooperativity of the hemes of cytochrome *c* oxidase as evidenced in the reaction with CO. *Arch. Biochem. Biophys.* 160:476–486.

Lyndsay, J. S., C. S. Owen, and D. F. Wilson. 1975. The invisible copper of cytochrome *c* oxidase, pH and AT dependence of its midpoint potential and its role in the oxygen reaction. *Arch. Biochem. Biophys.* 169:492–505.

Malmström, B. G. 1974. Cytochrome *c* oxidase: some current biochemical and biophysical problems. *Q. Rev. Biophys.* 6:389–431.

Naqui, A., C. Kumar, C. Yuan-Chin, L. Powers, and B. Chance, 1984. Structure and reactivity of multiple forms of cytochrome oxidase as evaluated by x-ray absorption spectroscopy and kinetics of cyanide binding. *Biochemistry.* 23:6222–6227.

Nicholls, P., and V. Hildebrandt. 1978., Binding of ligands and spectral shifts in cytochrome *c* oxidase. *Biochem. J.* 173:65–72.

Nicholls, P., and L. C. Petersen. 1974. Haem-haem interactions in cytochrome aa_3 during the anaerobic-aerobic transition. *Biochim. Biophys. Act.* 357:462–467.

Nicholls, P., and J. M. Wrigglesworth. 1988. Routes of cytochrome *a* reduction: the neoclassical model revisited. *Ann. NY Acad. Sci.* 550:59–67.

Okunuki, K., B. Hagihara, I. Sekuzu, and T. Horie. 1957. Studies on cytochrome oxidase. In *Proceedings of the International Symposium on Enzyme Chemistry.* Tokyo and Kyoto, Maruzen, Tokyo. K. Schihara, editor. Academic Press, Inc., New York. 264.

Reddy, K. V. S., and R. W. Hendler. 1986. Complete analysis of the cytochrome components of beef heart mitochondria in terms of spectra and redox properties: the c_1 cytochromes. *Biophys. J.* 49:693–703.

Reddy, K. V. S., R. W. Hendler, and B. Bunow. 1986. Complete analysis of the cytochrome components of beef heart mitochondria in terms of spectra and redox properties. Cytochrome aa_3. *Biophys. J.* 49:705–715.

Schroedl, N. A., and C. R. Hartzell. 1977. Oxidative titrations of reduced cytochrome aa_3: correlation of midpoint potentials and extinction coefficients observed at three major absorption bands. *Biochemistry.* 16:4961–4965.

Shrager, R. I., and R. W. Hendler. 1986. Processing and analysis of potentiometric data. *Biophys. J.* 49:687–691.

Steffens, G. C. M., R. Biewald, and G. Buse. 1987. Cytochrome *c* oxidase is a three-copper, two-heme-A protein. *Eur. J. Biochem.* 164:295–300.

Steffens, G. C. M., and G. Buse. 1988. Preliminary results of anaerobic titrations of bovine heart cytochrome *c* oxidase indicate the presence of five redox active metal centers. *Eur. Bioenerg. Conf. Rep.* 5:100.

Tiesjema, R. H., A. O. Muijsers, and B. F. van Gelder. 1973. Biochemical and biophysical studies on cytochrome *c* oxidase. X. Spectral and potentiometric properties of the hemes and coppers. *Biochim. Biophys. Acta.* 305:19–28.

Wever, R., J. H. Van Drooge, A. O. Muijsers, E. P. Bakker, and B. F. Van Gelder. 1977. The binding of carbon monoxide to cytochrome *c* oxidase. *Eur. J. Biochem.* 72:149–154.

Wever, R., J. H. Van Drooge, G. Van Ark, and B. F. Van Gelder. 1974. Biochemical and biophysical studies on cytochrome *c* oxidase. XVII. An EPR study of the photodissociation of cytochrome $a_3^{2+} \cdot$ CO. *Biochim. Biophys. Acta.* 347:215–223.

Wikström, M., H. J. Harmon, J. Ingledew, and B. Chance. 1976. A re-evaluation of the spectral, potentiometric and energy-linked properties of cytochrome *c* oxidase on mitochondria. *FEBS (Fed. Eur. Biochem. Soc.) Lett.* 65:259–277.

Wikström, M., K. Krab, and M. Saraste. 1981. Cytochrome oxidase, a synthesis. Academic Press, Inc., New York.

Wilson, D. F., and J. S. Leight. 1974. Heme-heme interaction between the cytochromes of the mitochondrial respiratory chain. *Ann. NY Acad. Sci.* 227:630–635.

Wilson, D. F., J. G. Lindsay, and E. S. Brocklehurst. 1972. Heme-heme interaction in cytochrome oxidase. *Biochim. Biophys. Acta.* 256:277–286.

Wrigglesworth, J. M., J. Elsden, A. Chapman, N. Van der Water, and M. F. Grahn. 1988. Activation by reduction of the resting form of cytochrome *c* oxidase: tests of different models and evidence for the involvement of Cu_B. *Biochim. Biophys. Acta.* 936:452–464.

Wrigglesworth, J. M., M. S. Wooster, J. Elsden, and H.-J. Daneel. 1987. Dynamics of proteoliposome formation. *Biochem. J.* 246:737–744.

Yonetani, T. 1961. Studies on cytochrome oxidase. III. Improved preparation and some proeprties. *J. Biol. Chem.* 236:1680–1688.

Yoshikawa, S., M. G. Choc, M. C. O'Toole, and W. S. Caughey. 1977. An infrared study of CO binding to heart cytochrome *c* oxidase and hemoglobin A. *J. Biol. Chem.* 252:5498–5508.

Yoshikawa, S., T. Tera, Y. Takahashi, T. Tsuikiharo, and W. S. Caughey. 1988. Crystalline cytochrome *c* oxidase of heart mitochondrial membrane. Composition and x-ray diffraction studies. *Proc. Natl. Acad. Sci. USA.* 85:1354–1358.